ARTICLE

Check for updates

Role of C$_4$ carbon fixation in *Ulva prolifera*, the macroalga responsible for the world's largest green tides

Dongyan Liu [1][✉], Qian Ma[1], Ivan Valiela[2], Donald M. Anderson[3], John K. Keesing [4], Kunshan Gao[5], Yu Zhen[6], Xiyan Sun[7] & Yujue Wang[1]

Most marine algae preferentially assimilate CO_2 via the Calvin-Benson Cycle (C$_3$) and catalyze HCO_3^- dehydration via carbonic anhydrase (CA) as a CO_2-compensatory mechanism, but certain species utilize the Hatch-Slack Cycle (C$_4$) to enhance photosynthesis. The occurrence and importance of the C$_4$ pathway remains uncertain, however. Here, we demonstrate that carbon fixation in *Ulva prolifera*, a species responsible for massive green tides, involves a combination of C$_3$ and C$_4$ pathways, and a CA-supported HCO_3^- mechanism. Analysis of CA and key C$_3$ and C$_4$ enzymes, and subsequent analysis of $\delta^{13}C$ photosynthetic products showed that the species assimilates CO_2 predominately via the C$_3$ pathway, uses HCO_3^- via the CA mechanism at low CO_2 levels, and takes advantage of high irradiance using the C$_4$ pathway. This active and multi-faceted carbon acquisition strategy is advantageous for the formation of massive blooms, as thick floating mats are subject to intense surface irradiance and CO_2 limitation.

[1] State Key Laboratory of Estuarine and Coastal Research, Institute of Eco-Chongming, East China Normal University, Shanghai 200062, China. [2] The Ecosystems Center, Marine Biological Laboratory, Woods Hole, MA 02543, USA. [3] Woods Hole Oceanographic Institution, Woods Hole, MA 02543-1049, USA. [4] CSIRO Oceans and Atmosphere Research, University of Western Australia Oceans Institute, Indian Ocean Marine Research Centre, Crawley, WA, Australia. [5] State Key Laboratory of Marine Environmental Science, Xiamen University, Xiamen 361005, China. [6] College of Environmental Science and Engineering, Ocean University of China, Qingdao 266100, China. [7] Muping Coastal Environment Research Station, Yantai Institute of Coastal Zone Research, Chinese Academy of Sciences, Yantai 264003, China. [✉]email: dyliu@sklec.ecnu.edu.cn

The Calvin–Benson cycle (C_3) is the dominant pathway of carbon fixation in marine algae[1]. Rubisco (ribulose-1, 5-bisphosphate carboxylase), a key C_3 enzyme responsible for carbon fixation, requires inorganic carbon in the form of CO_2[2]. However, the demand for CO_2 in algal photosynthesis is generally higher than CO_2 concentrations in natural seawaters, e.g., the half-saturation constants for CO_2 of Rubisco in diatoms are 30–60 μM[3] but CO_2 concentrations in natural seawater are only 5–25 μM[4]. Thus, CO_2 can be an important factor limiting algal proliferation in the ocean.

Since the 1970s there is growing evidence that most species of prokaryotic and eukaryotic algae have developed CO_2-concentrating mechanisms (CCMs) that enable accumulation of CO_2 via bicarbonate (HCO_3^-) enzymolysis[3,5]. A dominant route in the CCMs is that intra- or extracellular dehydration of HCO_3^- is catalyzed by carbonic anhydrases (CA) to release CO_2 to increase reactions at the Rubisco site (Fig. 1a). Although traditionally associated with more advanced terrestrial plants, in recent decades a C_4 or C_4-like pathway has been discovered in the green alga *Udotea flabellum*[6] and the marine diatom *Thalassiosira weissflogii*[7,8], in which transmembrane HCO_3^- is not only catalyzed via CA to generate CO_2 but also involves C_4 enzymes—phosphoenolpyruvate carboxylase (PEPCase) and PEPCase kinase (PEPCKase). CO_2 incorporated in this manner eventually enters the C_3 cycle to increase reactions at the Rubisco site (Fig. 1b). More recently, a freshwater macrophyte *Ottelia alismoides*, a constitutive C_4 plant and bicarbonate user, was shown to possess three different CCMs that can operate with the C_4 pathway in the same tissue, even though Kranz anatomy is absent[9,10]. Theoretically, the joint operation of CCMs and the C_4 pathway can greatly improve carboxylation efficiency of algal species in the use of HCO_3^-, and consequently enhance CO_2 accumulation at the Rubisco site (Fig. 1b).

Ulva prolifera, the main species involved in the massive "green tides" in the Yellow Sea[11], exhibits remarkable capability for biomass accumulation. *U. prolifera* biomass increases rapidly—more than 60-fold within ~50 days[12,13]. Growth rates in the field were generally higher than 28% per day at temperatures greater than 20 °C[14], and aerial cover of floating canopies exceed 30,000 km² across the Yellow Sea. Consistent with this, the involvement of the C_4 pathway in photosynthesis of *U. prolifera* has been suggested as an important mechanism to achieve such rapid biomass accumulation, based on two lines of evidence: (1) gene and enzyme analysis in *U. prolifera* revealed the existence and activity of the C_4-related enzyme pyruvate orthophosphate dikinase (PPDKase)[15]; and (2) tissue $\delta^{13}C$ range of *U. prolifera* (−21.9 to −14.9‰) at 16 stations in the Yellow Sea indicated a mix of C_3 and C_4 pathways in carbon fixation[16].

These two lines of evidence, however, are not sufficient to characterize a full C_4 pathway in *U. prolifera*. That pathway requires the participation of the key C_4 enzymes, PEPCase and PEPCKase. PEPCase (in the cytoplasm) supports catalysis of carboxylation of phosphoenolpyruvic acid (PEP), which uses HCO_3^- as the inorganic carbon substrate leading to C_4 compound synthesis. PEPCKase (in the chloroplast) is a decarboxylase, generating CO_2 and insuring efficient transfer of CO_2 to Rubisco[17]. PPDKase is responsible for catalyzing the regeneration of PEP in the cytoplasm, but it is not the only way for the C_4 pathway to acquire PEP[17]. Some researchers even believe that PPDKase might not assist with net CO_2 fixation but rather has a role in protection against photoinhibition[18]. Therefore, examining the activities of PEPCase and PEPCKase is a necessary step to confirm the existence of C_4 pathway in *U. prolifera*.

The $^{13}C/^{12}C$ distributions in plant tissue records the integrated pattern of photosynthetic carbon acquisition[19,20]; for example, high CO_2 uptake leads to low $\delta^{13}C$ values (e.g., <−30‰[21]), whereas high HCO_3^- uptake gives high $\delta^{13}C$ values (e.g., >−10‰[22]). Therefore, tissue $\delta^{13}C$ is an important index using to distinguish C_3 and C_4 activity. The $^{13}C/^{12}C$ values in seaweeds, however, often display a wide range that makes definition of the C_4 contribution uncertain[20,21]. The variation in the ratios depends on ambient temperature, light, salinity, nutrients and CO_2 concentrations in seawater[20,22]. Growth and respiration in seaweeds[20,23] can also lead to discrimination and fractionation of $^{13}C/^{12}C$. As canopies of *U. prolifera* drift in the Yellow Sea, environmental conditions and physiological activity change, forcing variations that may mask clear evidence for C_4 activity.

To resolve this uncertainty, controlled experiments are needed to examine the correlation between the activities of key enzymes and photosynthetic products to ascertain the activity
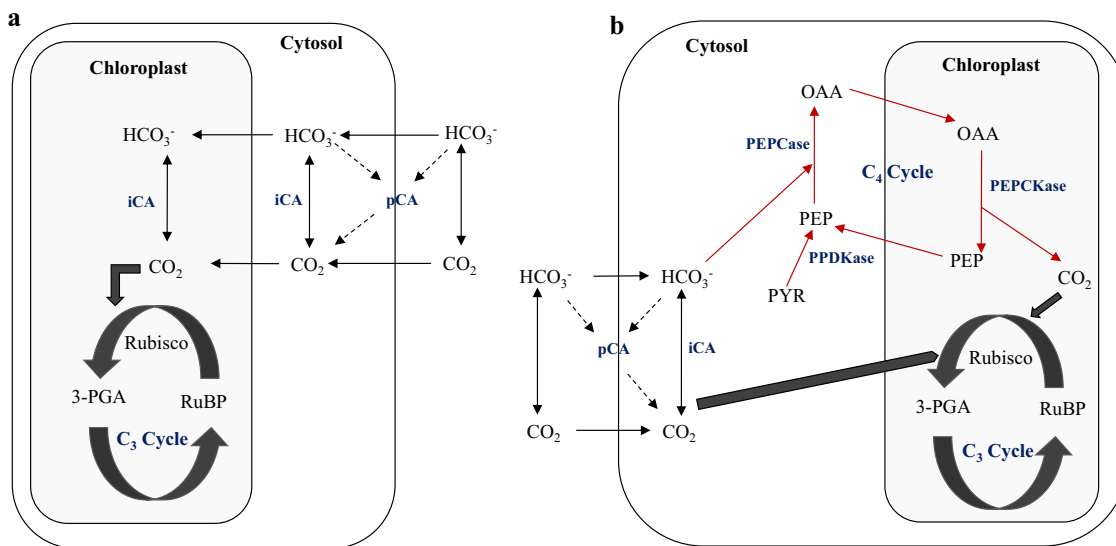

Fig. 1 Schematics of two carbon acquisition strategies in marine algae. a Transmembrane HCO_3^- is catalyzed by carbonic anhydrase (CA). **b** Transmembrane HCO_3^- is catalyzed by CA and the C_4 pathway (RuBP 1,2-ribulose diphosphate, 3-PGA 3-phosphoglyceric acid, pCA periplasmic (extra-cellular) CA, iCA intra-cellular CA, PEPCase phosphoenopyruvate carboxylase, PEPCKase phosphoenolpyruvate carboxylase kinase, PPDKase pyruvate orthophosphate dikinase, OAA oxaloacetic acid, PEP phosphoenolpyruvic acid, PYR pyruvic acid).
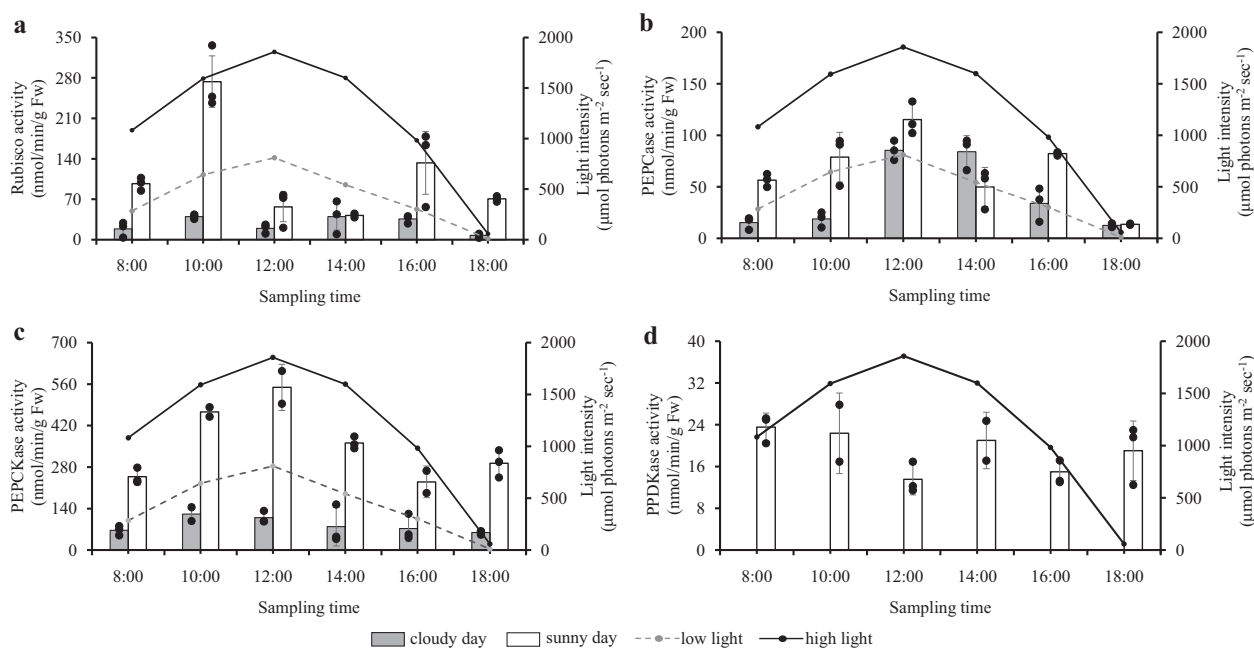
Fig. 2 Diurnal patterns of key C3 and C4 enzymes in *U. prolifera*, corresponding to variations in light intensity. a The pattern of C_3 enzyme (Rubisco) on sunny (experiment 1) and cloudy (experiment 2) days. **b–d** The pattern of C_4 enzymes on sunny (experiment 1) and cloudy (experiment 2) days. Each data bar is the mean of three measurements (black dots in each data bar are individual data points from each culture container) and error bars are ±1 standard deviation from the mean. Results of two-way analyses of variance comparing sunny and cloudy days were as follows: Rubisco comparison (all times excluding 18:00), light condition (cloudy/sunny) $F_{(1,20)} = 33.99$, $p < 0.0001$; time $F_{(4,20)} = 8.43$, $p = 0.0003$; light × time interaction $F_{(4,20)} = 6.25$, $p = 0.002$. PEPCase comparison (all times excluding 18:00), light condition $F_{(1,20)} = 32.74$, $p < 0.0001$; time $F_{(4,20)} = 18.38$, $p < 0.0001$; light × time $F_{(4,20)} = 10.64$, $p < 0.0001$. PEPCKase comparison (all times), light condition $F_{(1,20)} = 152.08$, $p < 0.0001$; time $F_{(5,20)} = 5.56$, $p = 0.002$; light × time $F_{(5,20)} = 2.48$, $p = 0.067$. See "Methods" for explanation of comparisons made and any transformations used.

of C_4 pathway and/or CA mechanism in *U. prolifera*. Although several environmental factors (e.g., temperature, light, salinity, HCO_3^- and CO_2 supply, and nutrient availability) may affect the functional expression and activity of CA mechanism and C_4 pathway, light intensity and pCO_2 are regarded as the most important two under the condition with sufficient nutrient supply[3,5,24]. Massive floating algal mats in nutrient enriched Yellow Sea are not only exposed to strong surface light, but the thick biomass also can reduce the dissolution of CO_2 from the air and lead to CO_2 limitation. Consequently, the HCO_3^- systems operated by CA mechanism and/or C_4 pathway would likely become active.

Here, we describe the results of three outdoor culture experiments designed to examine the daily variations of key C_3 (Rubisco), CA (extra- and intra-cellular CA) and C_4-metabolic enzymes (PEPCase, PEPCKase, and PPDKase) in *U. prolifera*. The relationships between the activities of major enzymes and photosynthetic products were analyzed via the corresponding variations in tissue $\delta^{13}C$, aiming to identify the participation of C_3 and C_4 photosynthetic pathways and CA mechanism in *U. prolifera*. The results exhibited the coexistence of C_3 and C_4 pathways and a CA-supported HCO_3^- mechanism in *U. prolifera*. The correlated variations of light intensity and pCO_2 with enzyme activity indicated that the C_4 pathway was most active under high light but that the CA mechanism became active at low CO_2 levels. The joint operation of the C_4 pathway and a CA-supported HCO_3^- mechanism in *U. prolifera* greatly improved efficiency of inorganic carbon fixation and illustrated why massive biomass accumulation can be formed in a short period, when thick floating mats are subject to intense surface irradiance and CO_2 limitation in the Yellow Sea.

Results

The response of key C_3 and C_4 enzymes to diurnal sunlight variations. The first two experiments showed that the activity of key C_3 and C_4 enzymes were much higher on a sunny day (experiment 1, Fig. 2) than on a cloudy day (experiment 2, Fig. 2). The patterns of C_3 and C_4 enzymes differed in response to variations in diurnal sunlight (Fig. 2): mean Rubisco activity was maximal in the morning (10:00 h) but declined significantly from 274 to 57 nmol · min^{-1} · g · fresh weight^{-1} at noon (12:00) under high light intensity (Tukey HSD = 5.327, crit. = 3.541, $p = 0.001$), and stayed low activity between 12:00 and 14:00 h, but increased significantly again from 42 to 143 nmol · min^{-1} · g · fresh weight^{-1} (Tukey HSD = 4.002, crit. = 3.541, $p = 0.019$) between 14:00 and 16:00 under reduced light intensity (Fig. 2a).

In contrast, PEPCase and PEPCKase activities reached maxima at noon, the time of peak irradiation (Fig. 2b, c). PEPCKase activity was significantly higher on the sunny day than on the cloudy day across all time periods from 08:00 to 18:00 (ANOVA, $F_{(1,20)} = 152.08$, $p < 0.0001$, Fig. 2c). PEPCase activity was significantly higher on the sunny day than on the cloudy day at three of the five time periods compared, 08:00, 10:00, and 16:00 (Tukey HSD = 3.634, 5.291, 4.253, respectively, crit. = 3.541, $p = 0.041$, 0.001, and 0.011, respectively, Fig. 2b). PPDKase to catalyze the regeneration of PEP in the C_4 pathway was only detected on sunny days (Fig. 2d). Regression analysis of enzyme activity against light (Fig. 3) confirm that high activity of C_4 enzymes (PEPCase [$R^2 = 0.544$, $p = 0.006$] and PEPCKase [χ^2 transformed, $R^2 = 0.651$, $p = 0.002$]) was induced under high irradiance. Rubisco ($R^2 = 0.244$, $p = 0.102$) did not display a linear relationship with light (Fig. 3). This is consistent with the results of the ANOVA above.
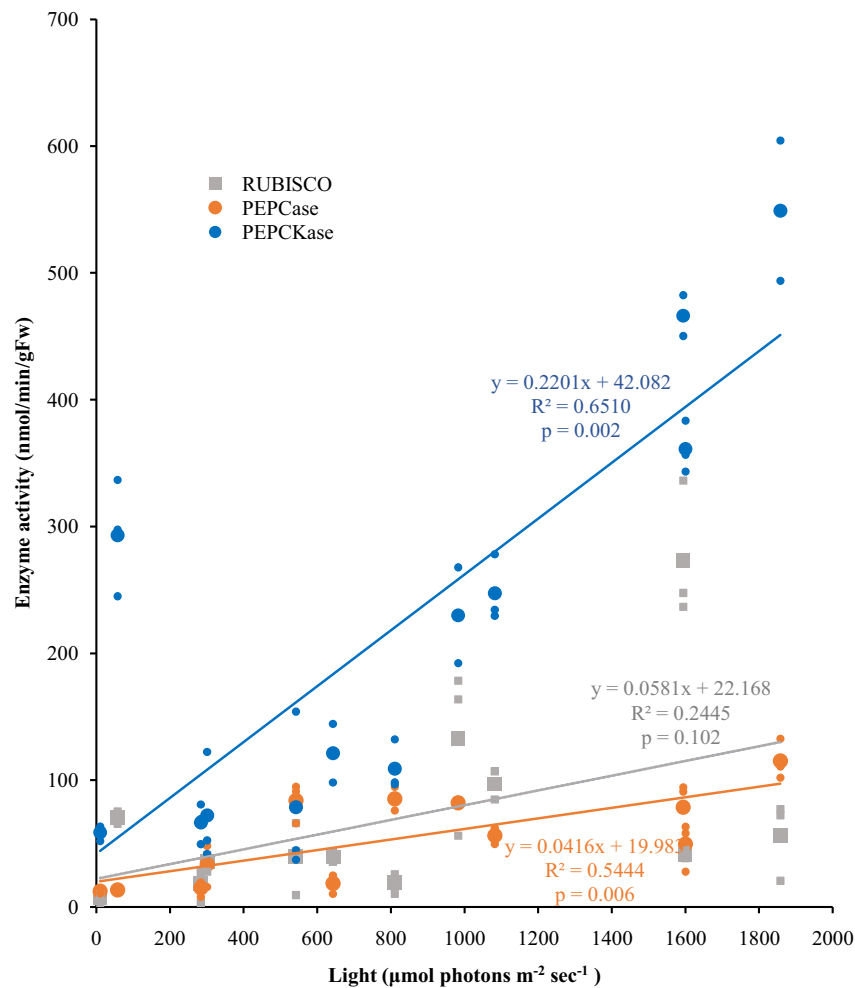
Fig. 3 Relationship between irradiance and enzyme activities for Rubisco, PEPCase, and PEPCKase. Means of three measurements (one from each culture container) of enzyme activity for each of 6 time periods in both sunny (experiment 1) and cloudy (experiment 2) days. Equations for regression lines shown are based on the plotted raw data (means: big color dots; individual data points: small color dots). R^2 and p values for PEPCKase are for the χ^2 transformed data as reported in the text. The R^2 and p value for the raw data were 0.6730 and 0.001, respectively.

Relationships between enzyme activities and carbon fixation.
The third experiment was conducted on a sunny day, aiming to identify the contribution of CO_2 and HCO_3^- in carbon fixation. The activities of key C_3 enzyme (Rubisco), C_4 enzymes (PEP-Case, PEPCKase, and PPDKase), and CA enzymes (extra- and intra-cellular CA) and their responses to varying light levels were measured over the course of the day (Fig. 4). Similarly, the variations of pCO_2, HCO_3^-, and tissue $\delta^{13}C$ were also measured (Fig. 5). The intent of this trial was to examine variations in key enzymes that represent the three photosynthetic routes, in relation to variations in photosynthetic products (tissue $\delta^{13}C$).

(1) Maximal Rubisco activity again occurred in the morning (Fig. 4a), along with rapidly decreased pCO_2 (Fig. 5a), and lowered tissue $\delta^{13}C$ (Fig. 5b). Photosynthesis during the morning was therefore dominated by a C_3 pathway supported by sufficient pCO_2 source.

(2) PEPCase and PEPCKase activities peaked at noon (Fig. 4b). From 10:00 to 12:00 as irradiance increased, tissue $\delta^{13}C$ increased 10‰ (Fig. 5b), suggesting a link between C_4 pathway and carbon fixation using HCO_3^-. The activity of PEPCase and PEPCKase and tissue $\delta^{13}C$ declined markedly at 2 p.m. (Fig. 4b), likely a result of decreased light intensity (Fig. 5b), consistent with the results from experiments 1

and 2, indicating the importance of strong light induction for C_4 pathway occurrence, rather than low pCO_2.

(3) Intra-cellular CA became more active in the afternoon (Fig. 4c) when pCO_2 was below 150 µatm (Fig. 5a). Throughout the experiment, the value of tissue $\delta^{13}C$ kept increasing after 2 p.m. (Fig. 5b), although the activities of PEPCase and PEPCKase declined markedly (Fig. 4b). Intracellular CA activity was negatively correlated to both pCO_2 ($R^2 = 0.773$, $p = 0.049$) and HCO_3^- concentration ($R^2 = 0.717$, $p = 0.070$), a result that indicated a CA-dominant photosynthetic pathway late in the day when pCO_2 decreased. In contrast, extracellular CA was not active and remained unchanged during the experiment (Fig. 5b), indicating the species mainly used the diffusion of HCO_3^- in cytosol via intracellular CA (Fig. 1b).

These results suggest that *U. prolifera* used a HCO_3^- source via a combination of C_4 pathways and the CA mechanism in response to changes in irradiation intensity and CO_2 level.

Discussion
The results of this study not only demonstrated the coexistence of C_3 and C_4 pathways and the CA mechanism in *U. prolifera* but also indicated that the C_4 pathway catalyzed by PEPCase and PEPCKase were most active in *U. prolifera* photosynthesis under
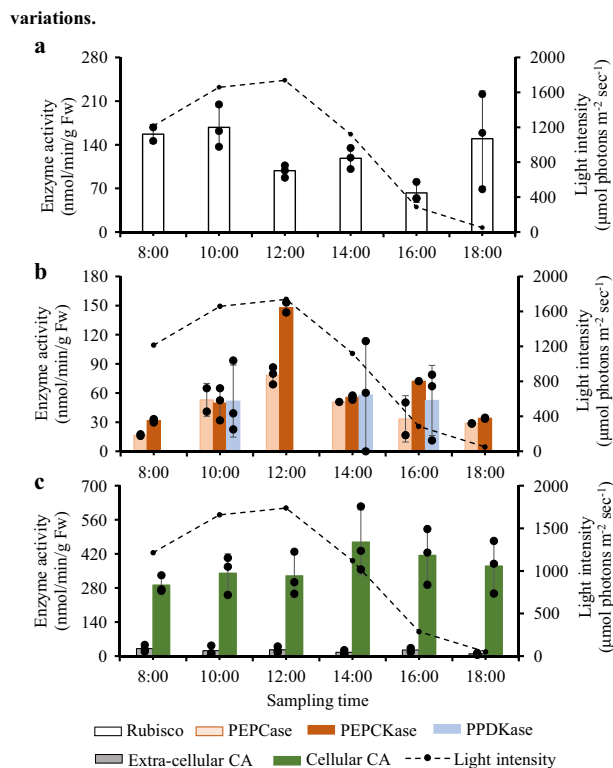
variations.

Fig. 4 Diurnal patterns of C3 and C4 enzymes and CA in response to sunlight variations. a Diurnal pattern of C_3 enzyme (Rubisco). **b** Diurnal patterns of C_4 enzyme (PEPCase, PEPCKase, and PPDKase). **c** Diurnal patterns of CA (extracellular and cellular CA). They indicate the activities of C_3 and C_4 pathways and CA mechanism, respectively, in response to diurnal sunlight variations. Each data bar is the mean of three measurements (one from each culture container) and error bars are ±1 standard deviation from the mean; black dots in each data bar are individual data points from each culture container.

Fig. 5 Diurnal variations of $pCO2$ and HCO3$^-$ concentrations and tissue δ^{13}C. a Diurnal variations of pCO_2 and HCO$_3^-$ concentrations in container seawater. **b** Diurnal variations in tissue δ^{13}C in *U. prolifera*. Each data point is the mean of three measurements from experiment 3, and the error bars are ±1 standard deviation from the mean (small black and orange dots in each error bar are individual data points from each culture container). Note that the decline in δ^{13}C between 08:00 and 10:00 indicates C_3 dominance, and thereafter, the decrease in δ^{13}C is indicative of C_4 dominance as pCO_2 declines below 200 µatm. Similarly, the decline δ^{13}C at 14:00 is associated with an increase in Rubisco (see Fig. 2a).

high light. In this regard, the photosynthetic machinery of *U. prolifera* could be similar to that previously described for the green alga *U. flabellum*[6] and the marine diatom *T. weissflogii*[8]. The CO$_2$ delivered to the Rubisco site comes from three sources: the available CO$_2$ from seawater, HCO$_3^-$ catalyzed by the CA mechanism, and HCO$_3^-$ catalyzed by PEPCase and PEPCKase via the C$_4$ pathway (Fig. 1b). The joint operation of the C$_4$ pathway and the CA mechanism greatly improve efficiency of inorganic carbon fixation in *U. prolifera*, and consequently, accelerate the rate of biomass accumulation (Fig. 1b). This multifaceted photosynthetic mechanism has important implications for the ability of this species to grow rapidly when there is high irradiance, and facilitates the formation of the massive floating green tide mats observed in the Yellow Sea[13].

Studies of the C$_4$ pathway in marine algal photosynthesis are very limited, but the results from a few species indicate that the occurrence of a C$_4$ pathway and its importance in carbon fixation have distinct species-specific expression. For example, inhibition of PEPCase or PEPCKase could reduce more than 90% of photosynthesis in *T. weissflogii*[8] and ~50% of photosynthesis in *U. flabellum*[6]. In this study, the range of tissue δ^{13}C (−19.1 to −17.4‰) implied an important contribution of HCO$_3^-$ in carbon fixation in *U. prolifera*. We cannot specifically define the contribution of HCO$_3^-$ fixed separately via the CA mechanism versus the C$_4$ pathway, but we found that the environmental factors inducing the activity of C$_4$ enzymes are different from the CA mechanism. The diurnal modalities of C$_4$ enzymes among the
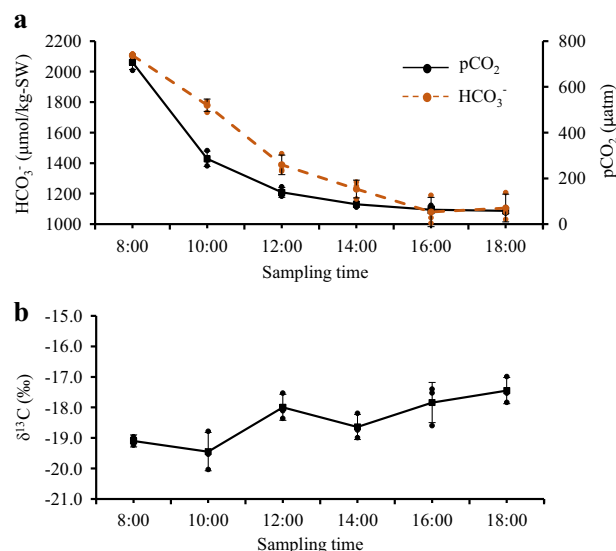
three experiments were consistent, although their concentrations were different depending on the ambient environmental conditions at the time of those experiments (Figs. 4 and 5). The repeated modes indicate that the highest PEPCKase activity occurred at maximal light (Figs. 2c and 4b); PEPCKase has a direct correlation with C$_4$ acid formation[6]. Previous studies on the diatom *T. pseudonana* also found that light intensity is more important for the C$_4$ acid accumulation than low pCO_2 concentrations[25,26]. In this study, tissue δ^{13}C showed a marked increase (10‰) at noon, indicating photosynthesis supported by HCO$_3^-$ (Fig. 5) and that the process is operated by C$_4$ pathway rather than C$_3$ pathway and CA mechanism (Fig. 4). In contrast, HCO$_3^-$ and CO$_2$ supply play important roles in modulating activity of C$_3$ pathway and CA mechanism[27]. High CO$_2$ generally suppresses expression of a high-affinity CCM state[28], a feature reflected in our result that the C$_3$ pathway was active at high pCO_2 concentrations but that the CA mechanism became dominant when pCO_2 was low (Figs. 4 and 5a).

HCO$_3^-$ transport rate and C$_4$ activity are energetically costly and require high photon flux densities and sufficient nutrient supply[29,30] to support synthesis of specific proteins. Excess light energy under strong irradiation however enables ATP to accumulate in the cells and leads to photoinhibition. An active C$_4$ pathway at noon indicates that *U. prolifera* has an efficient capability to dissipate excess light energy and ATP in cells. Photosystems I and II (PSI and PSII) are light-harvesting operators, and the energy flux they capture will be quenched and redistributed between PSII/PSI to achieve a balance and avoid irreversible damage to the photosynthetic systems[31]. An induction experiment with *U. prolifera* showed that the electron transport rate (ETR) between PSII/PSI was still high when light intensity reached 800 µmol photons m^{-2} s^{-1} [32]. Xu and Gao[33] found that the ETR and net photosynthetic rate of *U. prolifera* remain high and stable even as light intensity increased to 2000 µmol photons

$m^{-2} s^{-1}$. These results explain the continuous carbon accumulation of *U. prolifera* exposed to light intensity > 1200 µmol photons $m^{-2} s^{-1}$ for more than 2 h in sunny day experiments, which is about two- or threefold higher than that required to saturate the photosynthetic rate (600 µmol photons $m^{-2} s^{-1}$[33]). PPDKase might play an important role in dissipating excess energy and ATP in cells, since it is responsible for catalyzing the regeneration of PEP in the cytoplasm, where ATP is consumed during PEP formation from pyruvate (Fig. 1b). The basis for this speculation is from the experiments of Haimovich-Dayan et al.[18] who used RNA-interference to silence the single gene encoding PPDKase in *P. tricornutum* and found that the variations of PPDKase activity hardly affected net CO_2 fixation but were distinctly involved in dissipating excess energy and ATP in cells. In this study, we only detected PPDKase under sunny conditions, indicating its link with protection against photoinhibition. Based on our study and previous evidence, we propose that, of the three enzymes of C_4 metabolism, net CO_2 fixation in *U. prolifera* mainly is determined by PEPCase and PEPCKase, but energy dissipation depends on PPDKase.

Coastal eutrophication and high light supply in the Yellow Sea are important environmental conditions that favor the initiation of C_4 function of *U. prolifera*. During the summer (June–August) when the *U. prolifera* bloom is forming, dissolved inorganic nitrogen (DIN) concentrations are 10–80 µM near the coast and 1–15 µM offshore[16], and the average light intensity in surface seawaters is ~1072.2 µmol photons $m^{-2} s^{-1}$ [34]. In this study, the DIN concentrations in the culture medium were about 30 µM and the daily average light intensity on sunny days in experiments 1 and 3 was 1196 and 1011 µmol photons $m^{-2} s^{-1}$, respectively. These values fit within the range of environmental condition in the Yellow Sea. The pCO_2 supply is limited during the formation of green tide in the Yellow Sea, with a range of 300–450 µatm[35], and moreover, it can be affected by phytoplankton consumption. Large floating mats formed by *U. prolifera* block air–sea exchange, thus, HCO_3^- uptake and assimilation could become important for rapid biomass accumulation. This was reflected in the tissue $\delta^{13}C$ (culture samples: −19.5 to −17.4‰; field samples: −21.9 to −14.9‰)[16].

Ulva prolifera assimilates CO_2 predominately via the C_3 pathway, takes up HCO_3^- via the CA mechanism at low CO_2 levels, and takes advantage of high irradiation by deploying the C_4 pathway. This adaptive and multifaceted carbon acquisition strategy in *U. prolifera* is obviously an advantageous biological approach to support fast biomass accumulation and improve oxygen production in the filaments to sustain respiration for algae while floating in thick mats[36]. The relative contribution of the C_4 pathway and CA mechanism in utilizing the HCO_3^- system and the environmental thresholds that determine which of these pathways dominate at different stages of bloom development, maturity, and decline need to be further elucidated.

Ulva prolifera blooms are initiated from the biomass of thalli dislodged in the intertidal zone where the alga is subject to very high diurnal ranges in temperature and light and can tolerate partial desiccation[37]. Evolutionarily, the expression of C_4 photosynthesis in *U. prolifera* maybe an adaptive response that enables the species to take advantage of rapidly changing conditions, and which also leads to formation of unusual massive blooms. The ability to harness the benefit of C_4 photosynthesis might also be a feature of other types of blooming macroalga and warrants investigation.

Methods

Culture experiments. Floating specimens of *Ulva prolifera* were collected from the Yellow Sea and, after cleaning epiphytes off using sterilized seawater, the sampled thalli were cultured in a laboratory incubator for a week prior to the outdoor

experiments. Fifty grams of fresh thalli were placed into each of three replicate transparent plastic containers (53.5 cm × 39 cm × 32.5 cm), with 40 L of filtered seawater. To maintain ambient seawater temperatures in the containers, they were suspended in an outdoor seawater pond (60 × 100 m) at Muping Coastal Station of Chinese Academy of Sciences, China. Each experiment lasted 1 day from 08:00 to 18:00, without stirring. The first two outdoor culture experiments were carried out in July 2018, including a sunny day culture (experiment 1) and a cloudy day culture (experiment 2). The two experiments were to examine the responses of major enzyme activities of the C_3 and C_4 pathways (Rubisco, PEPCase, PEPCKase, and PPDKase) to diurnal variation of light intensity. The details are given below.

Algal sample was collected every 2 h from each of the three culture containers and stored in a liquid nitrogen tank prior to assays of enzyme activities. Light intensity, salinity, and air temperature were monitored during the culture using a light meter (TES-1339R, TES Electrical Electronic Corp., Taiwan), salinometer (S3-Standard kit, Switzerland), and thermometer (PT3003, Anymeter, China), respectively. The initial concentrations of DIN and dissolved inorganic phosphate (DIP) in the culture medium for both the sunny and cloudy day experiments were 34.6 and 0.67 µM, respectively. During experiments 1 and 2, salinity varied from 31.2 to 32.1 and water temperature was not much different on sunny (27.4–32.6 °C) versus cloudy (28.2–31.4 °C) days, but sunlight intensity was much higher on sunny days (57.5–1858 µmol photons $m^{-2} s^{-1}$) than cloudy days (10.2–810 µmol photons $m^{-2} s^{-1}$).

A third outdoor experiment (again with three replicate culture containers as described above) was conducted in August 2019 to define the correlation between major enzyme activities and corresponding photosynthetic products. This experiment was carried out on a sunny day, from 08:00 to 18:00. Samples were collected from each of the three culture containers every 2 h and stored in liquid nitrogen for the assays of enzyme activities and tissue $\delta^{13}C$. Meanwhile, the changes of pCO_2 and HCO_3^- were measured in the container seawater, and light, salinity, and air temperature were monitored through the day. The initial concentrations of DIN and DIP in the culture medium were 30.9 and 0.16 µM, respectively. During the third experiment, salinity varied from 33.1 to 33.8, water temperature ranged from 26.2 to 29.6 °C, and sunlight intensity from 50.4 to 1738 µmol photons $m^{-2} s^{-1}$.

Measurement of the pCO_2 and HCO_3^- concentrations. Twenty-five milliliters of water samples were taken from each of the three culture containers at each 2-h time interval and transferred to a fifty milliliters stoppered polyethylene bottle containing ten milliliters of a hydrochloric acid (HCl) standard solution (0.006 mol L^{-1}). After the pH in the water sample was stabilized, HCl standard solution was added into the sample to adjust the pH between 3.40 and 3.90. The added HCl volumes and pH values were recorded and total alkalinity calculated as

$$A = \frac{V_{HCl} \times c^{HCl}}{V_W} \times 1000 - \frac{a_{H^+} \times (V_W + V_{HCl})}{V_W \times f_{H^+}} 1000,$$

where A represents the alkalinity of the sample (mmol L^{-1}); c^{HCl} represents HCl standard solution (mol L^{-1}); V_W represents water sample volume (mL); V_{HCl} represents added HCl volume (mL); a_{H^+} represents the hydrogen ion activity corresponding to the solution pH; and f_{H^+} represents the hydrogen ion activity corresponding to the pH and actual salinity of the solution. All data, including temperature and salinity, were input into CO2SYS[38], which was used to calculate the pCO_2 and HCO_3^- concentrations.

Enzyme assays. The frozen algal samples were ground with liquid nitrogen, with ~0.1 g of the ground sample used for enzyme assays. The activities of Rubisco, PEPCase, and PPDKase were assayed using enzyme assay kits provided by Solarbio Life Sciences, China. The activity of PEPCKase was assayed using enzyme assay kits provided by Nanjing Jiancheng Bioengineering Institute, China. One unit of Rubisco, PEPCase, and PEPCKase activity is defined as the amount of enzyme consuming 1 nmol NADH per minute. One unit of PPDKase activity is defined as the amount of enzyme consuming 1 nmol NADPH per minute.

CA activity was assayed according to the method of Wilbur and Anderson[39]. Prior to storage in liquid nitrogen, ~0.1–0.14 g of fresh algal thallus (algal weight) were weighed and then soaked in 2 mL of barbiturate buffer (20 mmol/L, pH = 8.4). Five milliliters of CO_2-saturated water was injected to initiate the reaction. The reaction mixture was cooled in a 4 °C-water bath. The extracellular CA activity was assayed by measuring the time of catalyzed reaction required for the pH to change from 8.3 to 7.3 (T_c). The same procedure was repeated using 2 mL of barbiturate buffer without algal thallus and the uncatalyzed time required for background pH change from 8.3 to 7.3 was recorded (T_0). The extracellular CA activity was calculated according to the following formula: Enzyme activity (U/g) = ((T_0/T_c − 1) × 10)/algal weight.

Then, ~0.03–0.04 g of algal thallus was carefully ground in liquid nitrogen and soaked with 2 mL of barbiturate buffer (20 mmol/L, pH = 8.4) for the assay of total CA activity. The total CA activity was measured and calculated using the same method and formula as for extracellular CA activity. The intracellular CA activity was calculated by total CA activity minus extracellular CA activity.

Tissue δ¹³C measurement. After rinsing with 0.1 M HCl and washing with Milli-Q water, algal samples were freeze-dried and ground. Approximately 0.5–1 mg ground sample was placed into a 4×6 mm tin capsule for tissue $\delta^{13}C$ analysis. The samples were analyzed using an isotope-ratio mass spectrometer (MAT 253, Thermo Scientific, USA) at the Yantai Institute of Coastal Zone Research, Chinese Academy of Sciences. Reference gases were calibrated against International Reference Materials (IAEA-CH6, IAEA-600 and EMA-P1). Results are expressed relative to Vienna PeeDee Belemnite. Replicate measurements of a laboratory standard (acetanilide, Thermo Scientific) analyzed with the samples indicated that analytical errors were <0.1‰ for $\delta^{13}C$.

Statistics and reproducibility. Linear regression analysis was carried out to test the dependence of enzyme activity on irradiance levels using data from both the sunny and cloudy day experiments (experiments 1 and 2). Pearson's R^2 was used to determine the significance of the results. PEPCKase activity was transformed (χ^2) to ensure normality of residuals for the linear regression (Shapiro–Wilk test). Other variables did not require transformation. Two-way analyses of variance (ANOVA, factors = time of day and light condition) was carried out on data from experiments 1 and 2. These analyses compared the level of enzyme activity under sunny and cloudy conditions and between different time periods (three replicates at each time period). Comparisons for PEPCKase were made across all time periods from 08:00 to 18:00, and for Rubisco and PEPCase for time periods from 08:00 to 16:00. Bartletts test was used to check for homogeneity of variances. A square root transformation was required to correct the variance structure for Rubisco and PEPCase. The 18:00 time period was excluded for Rubisco and PEPCase as variance structure could not be corrected if it was included. Tukey's HSD was used for the pairwise comparisons. Correlation analyses were conducted on parameters measured in the third experiment for the time period from 08:00 to 14:00 (also three replicates) in order to examine the relationships between the activities of key enzymes and photosynthetic products to ascertain the activity of C_4 and/or CA pathways in *U. prolifera*. All analyses were undertaken using Addinsoft's statistical software XLSTAT.

Reporting summary. Further information on research design is available in the Nature Research Reporting Summary linked to this article.

Data availability

The data supporting the findings of this study and source data of main figures are provided as Supplementary Data.

References

1. Raven, J. A. Carbon dioxide fixation. in *Algal Physiology and Biochemistry* (ed Stewart, W. D. P.) 434–455 (Blackwell Scientific Publications, Oxford, 1974).
2. Cooper, T. G., Filmer, D., Wishnick, M. & Lane, M. D. The active species of "CO_2" utilized by ribulose diphosphate carboxylase. *J. Biol. Chem.* **244**, 1081–1083 (1969).
3. Badger, M. R. et al. The diversity and coevolution of Rubisco, plastids, pyrenoids, and chloroplast-based CO_2-concentrating mechanisms in algae. *Can. J. Bot.* **76**, 1052–1071 (1998).
4. Burkhardt, S., Amoroso, G., Riebesell, U. & Sültemeyerl, D. CO_2 and HCO_3^- uptake in marine diatoms acclimated to different CO_2 concentrations. *Limnol. Oceanogr.* **46**, 1378–1391 (2001).
5. Giordano, M., Beardall, J. & Raven, J. A. CO_2 concentrating mechanisms in algae: mechanisms, environmental modulation, and evolution. *Ann. Rev. Plant Biol.* **56**, 99–131 (2005).
6. Reiskind, J. B. & Bowes, G. The role of phosphoenolpyruvate carboxykinase in a marine macroalga with C_4-like photosynthetic characteristics. *Proc. Natl Acad. Sci. USA* **88**, 2883–2887 (1991).
7. Reinfelder, J. R., Kraepiel, A. M. L. & Morel, F. M. M. Unicellular C_4 photosynthesis in a marine diatom. *Nature* **407**, 996–999 (2000).
8. Reinfelder, J. R., Milligan, A. J. & Morel, F. M. M. The role of the C_4 pathway in carbon accumulation and fixation in a marine diatom. *Plant Physiol.* **135**, 2106–2111 (2004).
9. Shao, H. et al. Responses of *Ottelia alismoides*, an aquatic plant with three CCMs, to variable CO_2 and light. *J. Exp. Bot.* **68**, 3985–3995 (2017).
10. Han, S. et al. Structural basis for C_4 photosynthesis without Kranz anatomy in leaves of the submerged freshwater plant *Ottelia alismoides*. *Ann. Bot.* **125**, 869–879 (2020).
11. Liu, D., Keesing, J. K., Xing, Q. & Shi, P. World's largest macroalgal bloom caused by expansion of seaweed aquaculture in China. *Mar. Poll. Bull.* **58**, 888–895 (2009).
12. Keesing, J. K., Liu, D. Y., Fearns, P. & Garcia, R. Inter-and intra-annual patterns of *Ulva prolifera* green tides in the Yellow Sea during 2007–2009, their origin and relationship to the expansion of coastal seaweed aquaculture in China. *Mar. Poll. Bull.* **62**, 1169–1182 (2011).
13. Liu, D. et al. The world's largest macroalgal bloom in the Yellow Sea, China: formation and implications. *Estuar. Coast. Shelf Sci.* **129**, 2–10 (2013).
14. Zhang, J. H., Kim, J. K., Yarish, C. & He, P. The expansion of *Ulva prolifera* O. F. Müller macroalgal blooms in the Yellow Sea, PR China, through asexual reproduction. *Mar. Poll. Bull.* **104**, 101–106 (2016).
15. Xu, J. et al. Evidence of coexistence of C_3 and C_4 photosynthetic pathways in a green-tide-forming alga, *Ulva prolifera*. *PLoS ONE* **7**, e37438 (2012).
16. Valiela, I., Liu, D., Lloret, J., Chenoweth, K. & Hanacek, D. Stable isotopic evidence of nitrogen sources and C4 metabolism driving the world's largest macroalgal green tides in the Yellow Sea. *Sci. Rep.* **8**, 17437 (2018).
17. Hatch, M. D. C_4 photosynthesis: a unique blend of modified biochemistry, anatomy and ultrastructure. *Biochim. Biophys. Acta Rev. Bioenerg.* **895**, 81–106 (1987).
18. Haimovich-Dayan, M. et al. The role of C_4 metabolism in the marine diatom *Phaeodactylum tricornutum*. *N. Phytol.* **197**, 177–185 (2013).
19. O'Leary, M. H. Carbon isotopes in photosynthesis. *BioScience* **38**, 328–336 (1988).
20. Fry, B. $^{13}C/^{12}C$ fractionation by marine diatoms. *Mar. Ecol. Prog. Ser.* **134**, 283–294 (1996).
21. Carvalho, M. C. & Eyre, B. D. Carbon stable isotope discrimination during respiration in three seaweed species. *Mar. Ecol. Prog. Ser.* **437**, 41–49 (2011).
22. Cornwall, C. E. et al. Inorganic carbon physiology underpins macroalgal responses to elevated CO_2. *Sci. Rep.* **7**, 46297 (2017).
23. Carvalho, M. C., Hayashizaki, K. & Ogawa, H. Short-term measurement of carbon stable isotope discrimination in photosynthesis and respiration by aquatic macrophytes, with marine macroalgal examples. *J. Phycol.* **45**, 761–770 (2009).
24. Raven, J. A., Giordano, M., Beardall, J. & Maberly, S. C. Algal evolution in relation to atmospheric CO_2: carboxylases, carbon-concentrating mechanisms and carbon oxidation cycles. *Philos. Trans. Roy. Soc. B* **367**, 493–507 (2012).
25. Roberts, K., Granum, E., Leegood, R. C. & Raven, J. A. C_3 and C_4 pathways of photosynthetic carbon assimilation in marine diatoms are under genetic, not environmental control. *Plant Physiol.* **145**, 230–235 (2007).
26. Roberts, K., Granum, E., Leegood, R. C. & Raven, J. A. Carbon acquisition by diatoms. *Photosynth. Res.* **93**, 79–88 (2007).
27. Beardall, J. & Giordano, M. Ecological implications of microalgal and cyanobacterial CO_2 concentrating mechanisms, and their regulation. *Funct. Plant Biol.* **29**, 335–347 (2002).
28. Palmqvist, K., Yu, J. W. & Badger, M. R. Carbonic anhydrase activity and inorganic carbon fluxes in low- and high-Ci cells of *Chlamydomonas reinhardtii* and *Scenedesmus obliquus*. *Physiol. Plant.* **90**, 537–547 (1994).
29. Reinfelder, J. R. Carbon concentrating mechanisms in eukaryotic marine phytoplankton. *Ann. Rev. Mar. Sci.* **3**, 291–315 (2011).
30. Beardall, J. Effects of photon flux density on the CO_2-concentrating mechanism of the cyanobacterium *Anabaena variabilis*. *J. Plankton Res.* **13**, 133–141 (1991).
31. Kargul, J. & Barber, J. Photosynthetic acclimation: structural reorganization of light harvesting antenna-role of redox-dependent phosphorylation of major and minor chlorophyll *a/b* binding proteins. *FEBS J.* **275**, 1056–1068 (2008).
32. Zhao, X., Tang, X., Zhang, H., Qu, T. & Wang, Y. Photosynthetic adaptation strategy of *Ulva prolifera* floating on the sea surface to environmental changes. *Plant Physiol. Biochem.* **107**, 116–125 (2016).
33. Xu, J. & Gao, K. Future CO_2-induced ocean acidification mediates the physiological performance of a green tide alga. *Plant Physiol.* **160**, 1762–1769 (2012).
34. Li, J., Sun, X. & Zheng, S. In situ study on photosynthetic characteristics of phytoplankton in the Yellow Sea and East China Sea in summer 2013. *J. Mar. Syst.* **160**, 94–106 (2016).
35. Qin, B. Y., Tao, Z., Li, Z. W. & Yang, X. F. Seasonal changes and controlling factors of sea surface pCO_2 in the Yellow Sea. *IOP Conf. Ser.* **17**, 012025 (2014).
36. Krause-Jensen, D., McGlathery, K., Rysgaard, S. & Christensen, P. B. Production within dense mats of the filamentous macroalga *Chaetomorpha linum* in relation to light and nutrient availability. *Mar. Ecol. Prog. Ser.* **134**, 207–216 (1996).
37. Keesing, J. K., Liu, D., Shi, Y. & Wang, Y. Abiotic factors influencing biomass accumulation of green tide causing *Ulva* spp. on *Pyropia* culture rafts in the Yellow Sea, China. *Mar. Poll. Bull.* **105**, 88–97 (2016).
38. Pierrot, D., Lewis, E. & Wallace, D. W. R. *MS Excel Program Developed for CO_2 System Calculations. ORNL/CDIAC—105a.* (Carbon Dioxide Information Analysis Center, Oak Ridge National Laboratory, US Department of Energy, Oak Ridge, Tennessee, 2006).
39. Wilbur, K. M. & Anderson, N. G. Electronic and colorimetric determination of carbonic anhydrase. *J. Biol. Chem.* **176**, 147–154 (1948).

Author contributions

D.L. conceived and obtained support for the work, and led writing of the text; Q.M., Y.Z., and K.G. were responsible for the culture experiments and enzyme analysis; I.V., D.M.A., and J.K.K. contributed to data analyses, graphics, and manuscript drafting. X.S. and Y.W. supported for isotope analysis and sample pretreatments. All authors reviewed and approved the content of the manuscript.

Competing interests

The authors declare no competing interests.

Additional information

Supplementary information is available for this paper at https://doi.org/10.1038/s42003-020-01225-4.

Correspondence and requests for materials should be addressed to D.L.

Reprints and permission information is available at http://www.nature.com/reprints

Publisher's note Springer Nature remains neutral with regard to jurisdictional claims in published maps and institutional affiliations.